Red–green and achromatic temporal filters: a ratio model predicts contrast-dependent speed perception

Andrew B. Metha and Kathy T. Mullen

McGill Vision Research, Department of Ophthalmology (H4-14), McGill University, 687 Pine Avenue West, Montreal, Quebec H3A 1A1, Canada

Received June 28, 1996; revised manuscript received November 20, 1996; accepted December 2, 1996

We simultaneously measured detection and identification performance by using isoluminant red–green (RG) and achromatic flickering stimuli and fitted these data with a modified line-element model that does not make high-threshold assumptions. The modeling shows that detection and identification data are adequately described by postulating only two underlying temporal filters each for RG and achromatic vision, even when more than two threshold classifications are evident. We use a spatial frequency of 1.5 cycles per degree (c/deg) and compare the derived temporal impulse response functions with those obtained previously with the use of 0.25-c/deg stimuli under otherwise identical conditions [J. Opt. Soc. Am. A **13**, 1969 (1996)]. We find that at 1.5 c/deg the luminance impulse response functions peak later and integrate out to longer times compared with those measured at 0.25 c/deg. For RG stimuli, although their relative overall sensitivities change, the impulse response functions are similar across spatial frequency, indicating a constancy of chromatic temporal properties across spatial scales. In a second experiment, we measured RG and achromatic flicker discrimination over a wide range of suprathreshold contrasts. These data suggest a common nonlinear contrast response function operating after initial temporal filtering. Using a ratio model of speed perception in which both RG and achromatic filters are combined at a common motion site, we can predict (1) the perceived slowing of RG stimuli compared with the perceived drift of achromatic drifting stimuli, (2) the contrast dependency of speed perception for RG and achromatic drifting stimuli, and (3) how this dependency changes with base speed. Thus we conclude that there is no need to postulate separate mechanisms for fast and slow motion [Nature (London) **367**, 268 (1994)], since a unified ratio model can explain both RG and achromatic contrast–speed dependency. © 1997 Optical Society of America [S0740-3232(97)02205-9]

Key words: color, luminance, isoluminance, temporal frequency, flicker, detection, identification.

1. INTRODUCTION

Using an analysis of detection threshold and temporal-frequency (TF) identification performance, we have previously reported[1] that the temporal properties of the chromatic red–green (RG) system at coarse spatial scales [0.25 cycle per degree (c/deg)] comprise more than a single underlying temporal filter. This finding parallels the generally held assertion that a small number of broadly tuned TF filters also underlie luminance vision[2–4] and are assumed to provide low-level input to the luminance motion pathway.[5–8] Likewise, for luminance vision, multiple spatial-frequency-tuned filters are generally thought to underlie the spatial contrast sensitivity function (see Ref. 9 for a review). Recent psychophysical evidence also points to the existence of multiple spatial channels in the RG chromatic system,[10,11] although the temporal properties of these chromatic channels and how they relate to motion processing remain largely unexplored. Thus the RG and luminance spatiotemporal contrast sensitivity surfaces for human vision, which are inseparable when considered as a whole (although see Yang and Makous[12] for an alternative view), appear to be tiled by an ensemble of locally tuned spatiotemporal filters. One issue of theoretical concern is the nature of this tiling, especially whether the temporal filtering properties among the spatial filters are constant across spatial scales. Another issue concerns how these filters may be subsequently used in the visual system to construct mechanisms sensitive to the speed and the direction of chromatic and achromatic visual information.

The aims of this paper are twofold. In the first experiment, we examine to what extent the temporal properties of the RG and luminance systems are preserved across spatial scales. To do this, we have undertaken an analysis of detection and TF identification by using near-threshold isoluminant RG and achromatic stimuli at a spatial frequency of 1.5 c/deg, enabling us to compare results with previous data obtained at 0.25 c/deg.[1] Using the same modeling procedure as that in Ref. 1, which assumes that the RG and achromatic detection performances are each based on probability summation over time from the output of two statistically independent temporal filters and that identification performances are based on the distribution of these filter responses with respect to a line-element criterion in a common internal response space, we derive best-fitting impulse response functions for the two subsystems. This information allows us to compare the temporal properties of the RG and luminance systems at two widely different spatial scales (a factor of 6 apart).

We have also previously shown[1] how, within this model framework, the differences in the front-end linear filters

0740-3232/97/050984-13$10.00

subserving the RG and luminance systems may account for the well-known perceived slowness of RG isoluminant stimuli compared with that of achromatic stimuli moving at the same physical speed.[13,14] The model, however, is based on threshold performance data, which, while providing good information about the nature and the absolute sensitivities of the temporal filters, leave unexplored how the system operates at (more normally encountered) suprathreshold contrast levels. Following from this, the second aim of this paper is to investigate how each filter is transduced as a function of contrast, a factor that is not well constrained by detection threshold and identification data alone. Physiological recordings of individual neuron contrast response functions are usually monotonic and saturate at some contrast level depending on the type of neuron and the stage of the visual system in which they reside.[15] Given that a mechanistic approach to the visual system must ultimately be based on neural elements, we would expect that the filters that we abstractly describe should also display properties of saturation. This has important bearings on the predictions of the model when it is used to compute speed estimates and to calculate how these depend on contrast. As noted by Adelson and Bergen,[7] when the filter outputs all pass through common power functions, their response ratios will remain fixed as contrast is varied, and computed speed derived from a ratio model will be strictly contrast invariant. However, there are now several studies in the literature reporting that this is not the case and that both chromatic and achromatic perceived speeds are contrast dependent.[14,16–19] Thus a linear or power transduction process is insufficient to explain these results. It has been proposed by ourselves[1] and others[20] that different power transducers applied separately to the underlying temporal filters may be invoked to explain this discrepancy—this paper presents an even simpler solution.

As well as determining how perceived speed may depend on contrast type (RG or achromatic) and level, the transduction properties of the initial filters also affect the predictions of the line-element model for the accuracy of suprathreshold TF discrimination. In the second experiment, we test flicker discrimination performance from two base frequencies for both RG and achromatic stimuli as a function of contrast and use these data to constrain the form of the filter contrast response function. We demonstrate that a ratio model that incorporates this form of transducer function can predict the contrast–speed dependency reported in the literature.[14,16–19]

2. METHODS

A. Subjects and Stimuli

The two authors served as subjects, who observed monocularly at a distance of 180 cm from the CRT face under dim ambient room illumination. A small fixation marker (2-mm-diameter black spot) centered on the screen aided fixation. Both subjects had normal color vision. KTM wore her prescribed corrective spectacles; ABM's tested eye was emmetropic.

The stimuli were cardinal RG or achromatic sinusoidal counterphase-flickering Gabor patches of 1.5 c/deg. These were generated by a digital waveform generator (Cambridge Research Systems VSG 2/2) and presented on a Barco Calibrator CCID 775 RGB monitor, with frame rate of 120 Hz. The mean chromaticity (1931 CIE: $x = 0.3377$, $y = 0.3184$) and luminance (62.2 cd/m^2) of the display were not altered by the presentation of the stimuli, which were ramped on and off in contrast according to a raised cosine profile with total duration of 1 s, resulting in a TF bandwidth of 0.76 Hz (equivalent Gaussian standard deviation) centered on the sinusoidal modulation frequency for each stimulus. TF's ranged from 1 to 16 Hz for the RG stimuli and from 1 to 32 Hz for the achromatic stimuli. Spatial windowing was also applied by a Gaussian contrast envelope with standard deviation of 0.66°, truncated at a total stimulus diameter of 2.64° that included 4 cycles of the sinusoidal grating. The vertical profile of the stimuli had 12-bit resolution, while the horizontal profile was generated by using frame-by-frame dynamic dithering of 12 statistically independent 1-bit Gaussian masks (pixel size 0.54 × 0.54 mm).[21] The screen display size was 35.4 cm × 26.2 cm. Calibration and gamma correction are described elsewhere.[22]

The cone contrast weights to the luminance postreceptoral mechanism are not fixed but depend on individual observer differences,[23] the state of chromatic adaptation,[24,25] and the TF content of the stimulus.[21,26,27] We thus used a minimum-motion paradigm and method of adjustment to determine the RG isoluminance direction for each TF tested for each observer.[27] A suprathreshold stimulus modulating L- and M-cone contrast equally but in spatial *antiphase* was continuously presented to the observer, drifting at the test TF. The observer adjusted the contrast of a superimposed drifting L- and M-cone *in-phase* stimulus until a percept of minimum motion was attained. The resulting stimulus defines the RG cardinal (isoluminant) direction.

Figure 1 shows the L:M cone contrast contribution ratio to the luminance mechanism derived from the isolumi-

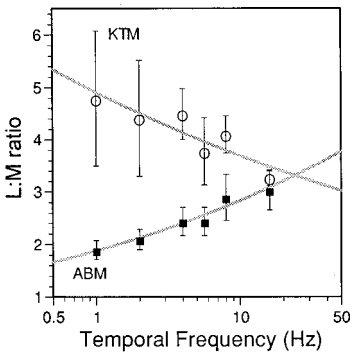

Fig. 1. RG cardinal cone contrast ratios as a function of temporal frequency (TF) for KTM (open circles) and ABM (filled squares). Each point represents the mean of ten minimum-motion settings in the L–M plane of cone contrast space; the error bars indicate one standard deviation. The curves are the best-fitting power functions to the data, which were used as templates in experiment 2 [for ABM, L:M = $1.8844 \times \mathrm{TF}^{0.1776}$ ($r^2 = 0.957$); for KTM, L:M = $4.9125 \times \mathrm{TF}^{-1.2385}$ ($r^2 = 0.788$)].

nance settings for both observers as a function of TF; the error bars represent the standard deviation of ten minimum-motion settings. The larger error bars shown for observer KTM are a reflection of the closeness of the RG cardinal direction to the M-cone contrast axis and do not imply that this observer had any more variability in making minimum-motion settings. As found previously by using 0.25-c/deg stimuli,[1] the L:M ratio varies significantly and in opposite directions for the two observers as a function of TF. The curves shown in Fig. 1 are the best-fitting power functions to these data, which were used to determine the appropriate isoluminance ratios when intermediate TF's were used. We assume that the luminance cardinal direction is one that excites L, M, and S cones equally and in phase, resulting in a stimulus whose chromaticity is not different from the adapting background.

A stimulus in a cardinal direction in color space should excite only one postreceptoral mechanism. However, there is psychophysical[28,29] and electrophysiological[30–32] evidence suggesting that, at least for stimuli containing low-spatial-frequency information, luminance mechanisms may play some role in detection of nominally RG isoluminant high-TF stimuli by means of the frequency-doubled responses of retinal M-pathway neurons. Other evidence, however, suggests that this intrusion is not necessarily present.[1,33]

Although band-limited 1.5-c/deg stimuli were used here, in order to ensure that the high-TF nominally isoluminant chromatic condition involved the activation of an intruding luminance mechanism, we performed simultaneous color detection and identification measurements at the two highest TF's (8 and 16 Hz) for both subjects. This allows us to examine objectively the nature of the chromatic percept at detection threshold.[34,35] If only the RG mechanism was involved in RG stimulus detection, then the stimulus should appear chromatic (red and green) at detection threshold. In a method analogous to the TF identification procedure described below, we determined detection and color identification performance by using randomly intermixed achromatic and nominally isoluminant stimuli, each at five contrast levels spanning detection threshold. If an intruding luminance mechanism mediates detection for both achromatic and nominally isoluminant stimuli, then correct color identification will not be possible at detection threshold.

We found that at both 8 and 16 Hz, color identification performance closely followed detection performance for both observers. The average separations between detection and color identification thresholds (±estimated standard deviation) were as follows: for KTM, 0.072 ± 0.022 (8 Hz) and 0.002 ± 0.029 $\log_{10}$ unit (16 Hz); and for ABM, 0.044 ± 0.036 (8 Hz) and 0.018 ± 0.059 $\log_{10}$ unit (16 Hz). These very small differences in detection and identification thresholds confirm that separate *chromatic* and *luminance* mechanisms mediate performance for the cardinal RG and achromatic stimuli, respectively, even at the highest flicker rates used in this study.

B. Procedures for Experiment 1

Detection and identification performances were measured simultaneously for pairs of different TF stimuli as a function of contrast by using a 2×2-interval forced-choice procedure. RG and achromatic stimuli were tested separately. Discrimination between all 15 pairs of TF's in the set 1, 2, 4, 5.66, 8, and 16 Hz for RG stimuli and the set 1, 2, 4, 8, 16, and 32 Hz for achromatic stimuli was measured. Initially, interleaved staircases were run to determine the threshold contrasts of each stimulus pair. Five contrast levels were then chosen to span each frequency's detection threshold, and the resulting ten stimuli were used in a method of constant stimuli experiment. Each trial of the experiment consisted of two 1.0-s intervals, separated by 0.5 s and marked by tones. One TF was randomly presented in one of the intervals, at one of the five near-threshold-contrast levels. The other interval was a blank. Observers responded with two button presses: First, they indicated in which interval the stimulus appeared (detection task); and second, they indicated whether the stimulus was the faster or the slower of the frequencies under consideration (identification task). Feedback was given after each response, and the ten stimuli were presented 40 times each. Because the contrasts used in the experiment straddle detection threshold for both TF's and were randomly intermixed, stimulus contrast could not be used to aid identification of the stimulus that was presented in any one trial.

C. Procedures for Experiment 2

Experiment 2 is closely related to experiment 1 but turns the question around. Instead of asking how much contrast must be increased above detection threshold to permit correct classification of two frequencies, we ask how close two frequencies can become while still remaining distinguishable, at a wide range of seven (ABM) or eight (KTM) suprathreshold contrast levels. Four conditions were explored for each observer with the use of cardinal RG and achromatic stimuli at base frequencies of 2 and 5.66 Hz. A stimulus appeared in each interval of a 2 -interval forced-choice trial: One of these flickered at a base TF (2 or 5.66 Hz), and the other flickered at the base frequency plus some increment (base TF + ΔTF). The observer's task was to indicate by button press the interval containing the higher TF. For low-contrast stimuli (and also the near-threshold stimuli used in experiment 1), the observers found that they could not adopt the strategies of actually counting the number of cycles presented or attending to the phase at which the visible stimulus begins and ends in order to perform the discrimination task. Nonetheless, these cues are potentially available for discrimination of the higher-contrast stimuli. In practice, however, observers found that the number of cycles during the 5.66-Hz base condition could not be counted and that the phase cues are largely eliminated by the raised cosine temporal contrast envelope for both 2- and 5.66-Hz conditions. The resulting data (shown in Fig. 5 below) also rule out the use of cycle counting in the 2-Hz condition because the final threshold frequency differences were substantially less than 1 cycle in all cases. Moreover, observers reported that they were attending to flicker speed *per se* while performing the discrimination task. In order to minimize any possible contrast cues in

the discrimination task arising from TF and TF + ΔTF having different contrast levels in terms of multiples of threshold, we adjusted the contrast of the faster stimulus according to the contrast sensitivity function given in each condition in Fig. 2. Similarly, as shown in Fig. 1, the cardinal L:M ratio for the RG stimuli was adjusted to ensure isoluminance according to a template as ΔTF was varied by the staircase procedure. As an added precaution against the use of associated contrast cues in the discrimination task, the contrast of each stimulus was also randomly jittered by up to 0.05 $\log_{10}$ unit.

A staircase controlled the size of ΔTF such that when two sequential correct responses were made, ΔTF was decreased by 0.1 $\log_{10}$ unit. After each incorrect response, ΔTF was increased by the same amount. Each staircase converges on the 71% correct discrimination level, and the geometric mean of the final six reversals was recorded. Measurements at all contrast levels were interleaved in a single experimental block, which was repeated 6–8 times for each observer. The average and the standard deviation of the ΔTF thresholds were calculated for each condition.

3. RESULTS

A. Experiment 1: Detection and Identification Psychometric Functions

Each detection–identification experiment yields four psychometric functions (one detection and one identification function for each TF). These psychometric curves were simultaneously fitted with base-2 Weibull functions by a least-chi-square procedure using the estimated binomial standard deviations at each point as weight factors.[1] The 75% detection threshold parameters were used as a measure of threshold of the RG and luminance mechanisms. To calculate sensitivities, we need to take into account the projection of the cardinal stimuli onto their respective *mechanism directions* (the direction in cone contrast space that optimally excites each postreceptoral mechanism). Because the RG cardinal direction changes with TF (Fig. 1), these projections also change, and the RG and luminance sensitivities reported here are adjusted accordingly.

1. Detection Performance

Figure 2 shows the sensitivities of the achromatic and RG

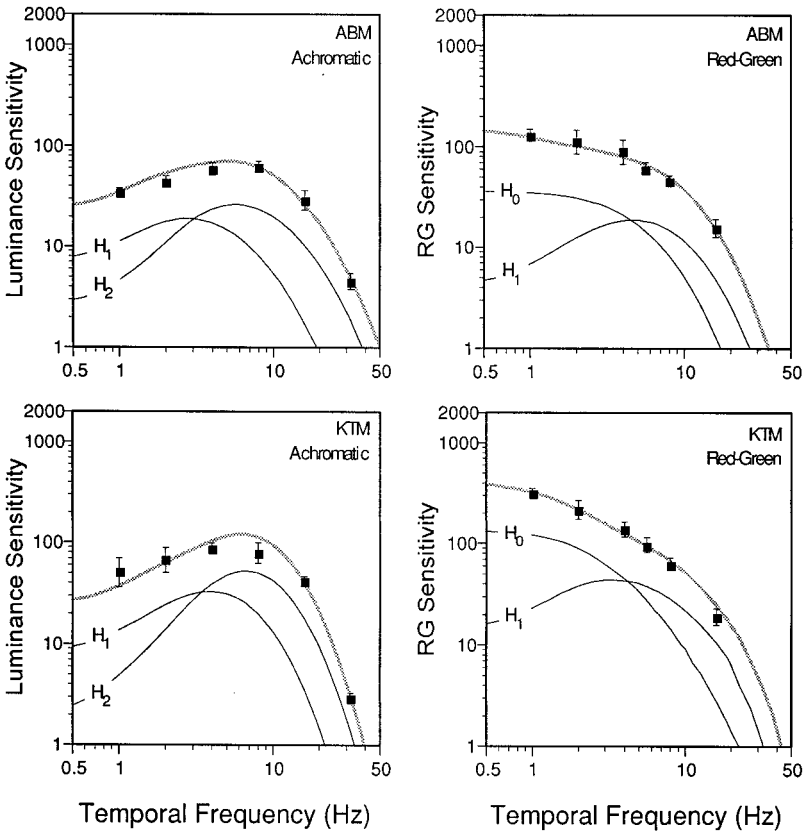

Fig. 2. Temporal cone contrast sensitivity functions for both observers measured with the use of achromatic (left) and RG isoluminant (right) stimuli. The filled squares represent the mean and the standard deviation of the five detection thresholds determined for each TF during the 2 × 2-interval forced-choice comparison sessions in experiment 1. The thick gray curves represent the model predictions for detection performance after parameters were adjusted to give the best fit for both detection and identification data. The thin curves are the modulation transfer functions of the inferred filters underlying the luminance and RG mechanisms. Figure 1 shows that the luminance mechanism receives varying L- and M-cone contrast input as a function of TF; therefore luminance sensitivity is given here as the reciprocal (in cone contrast units) of the threshold achromatic cardinal stimulus projection onto the measured luminance mechanism for each TF. RG sensitivity is given as the reciprocal of the threshold isoluminant stimulus projection onto the RG mechanism, which we assume receives fixed (equal and opposite) L- and M-cone contrast input at all TF's.

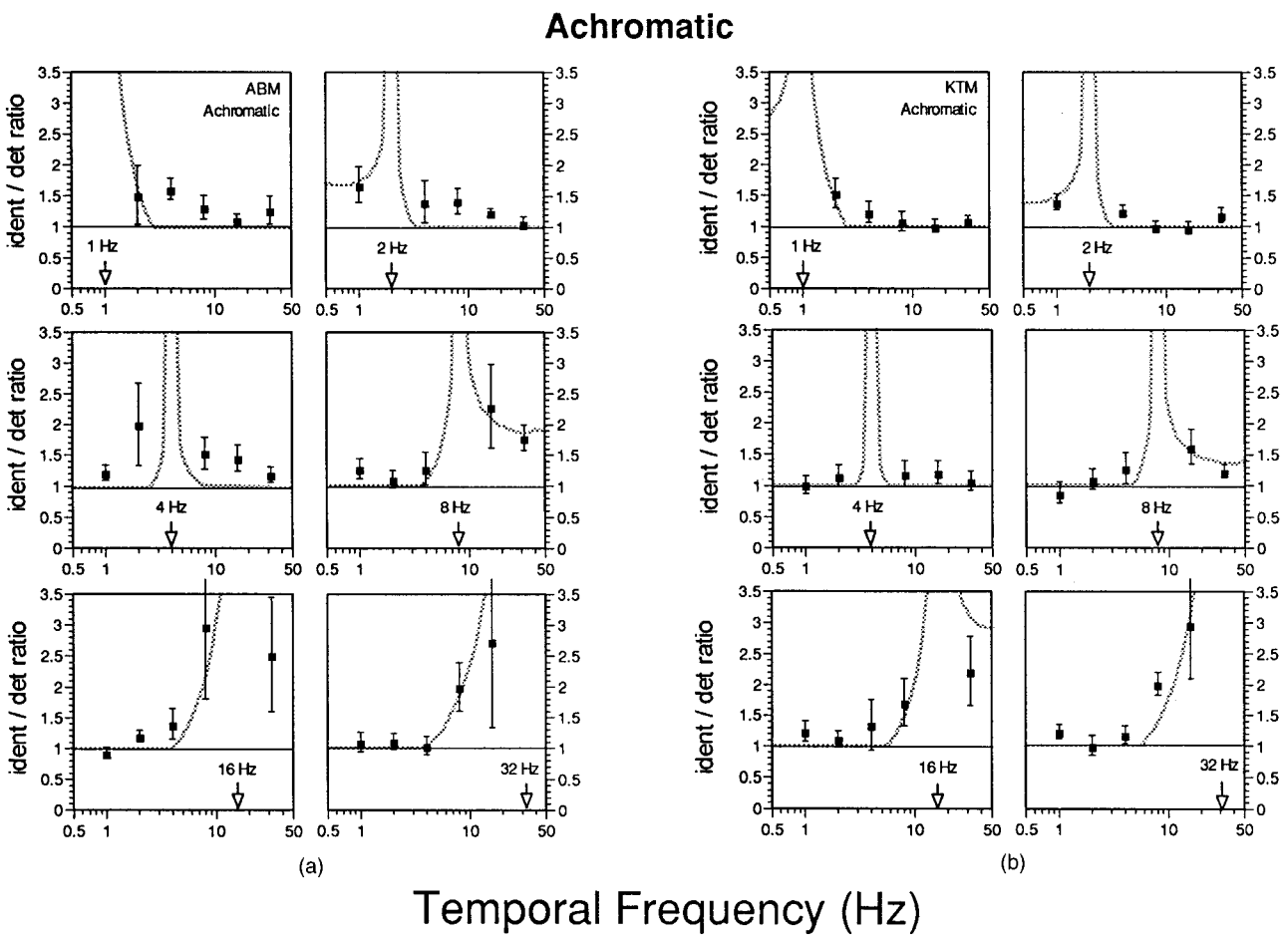

Fig. 3. Continues on facing page.

mechanisms, plotted as cone contrast sensitivity versus TF on log–log axes. Because sensitivity is plotted in cone contrast units, the luminance and RG mechanisms can be compared directly. Results for the two observers are very similar. As is typically found for low-spatial-frequency stimuli, the luminance temporal contrast sensitivity function displays a bandpass shape, with sensitivity peaking between 4 and 8 Hz. The temporal contrast sensitivity function for stimuli isolating the RG mechanism displays a characteristic low-pass shape. Below 5.66 Hz we find that the RG mechanism is more sensitive than the luminance mechanism for each observer at 1.5-c/deg. With the use of 0.25-c/deg stimuli, this crossover occurred at approximately 8 Hz.[1] Thus there is a relative increase of the luminance mechanism sensitivity over that of the RG mechanism as spatial frequency increases, as would be expected from the characteristic spatial contrast sensitivity functions described in the literature.[36] The thick gray curves in Fig. 2 represent the detection performance predicted by the model described in Subsection 3.B, based on the inferred underlying temporal filters, whose modulation transfer functions are shown by thin curves. In agreement with the results for 0.25-c/deg stimuli,[1] the RG data are best modeled by using impulse response functions that have the form of a log-time Gaussian and its first derivative, while the achromatic data are best fit by using the first and second derivatives of a log-time Gaussian. Attempts to model the data by using other combinations of independent filters, for example orthogonal bandpass and low-pass filters for the achromatic data, resulted in poorer fits (see Ref. 1 for further details). One should note, however, that the achromatic low-frequency bandpass filter has a very shallow low-TF limb and is comparable with the filter shapes found by others using masking studies.[3,6,8] The large gap between the underlying filter curves and the overall sensitivity shown in Fig. 2 reflects the increase in sensitivity gained by the operation of probability summation over time. It must be remembered that these fits are not based on detection data alone but also take into account the near-threshold TF identification data.

2. *Identification Performance*

From each method of constant stimuli experiment, we compare identification and detection performance by dividing the 75% identification threshold by the 75% detection threshold estimates. This provides a measure of how much contrast must be raised above detection threshold level to yield 75% identification performance, giving an identification/detection threshold ratio. By considering the standard deviations of the detection and identification threshold estimates from the Weibull fits as independent Gaussian variables, we also derive an estimate for the standard deviation of each measured threshold ratio.

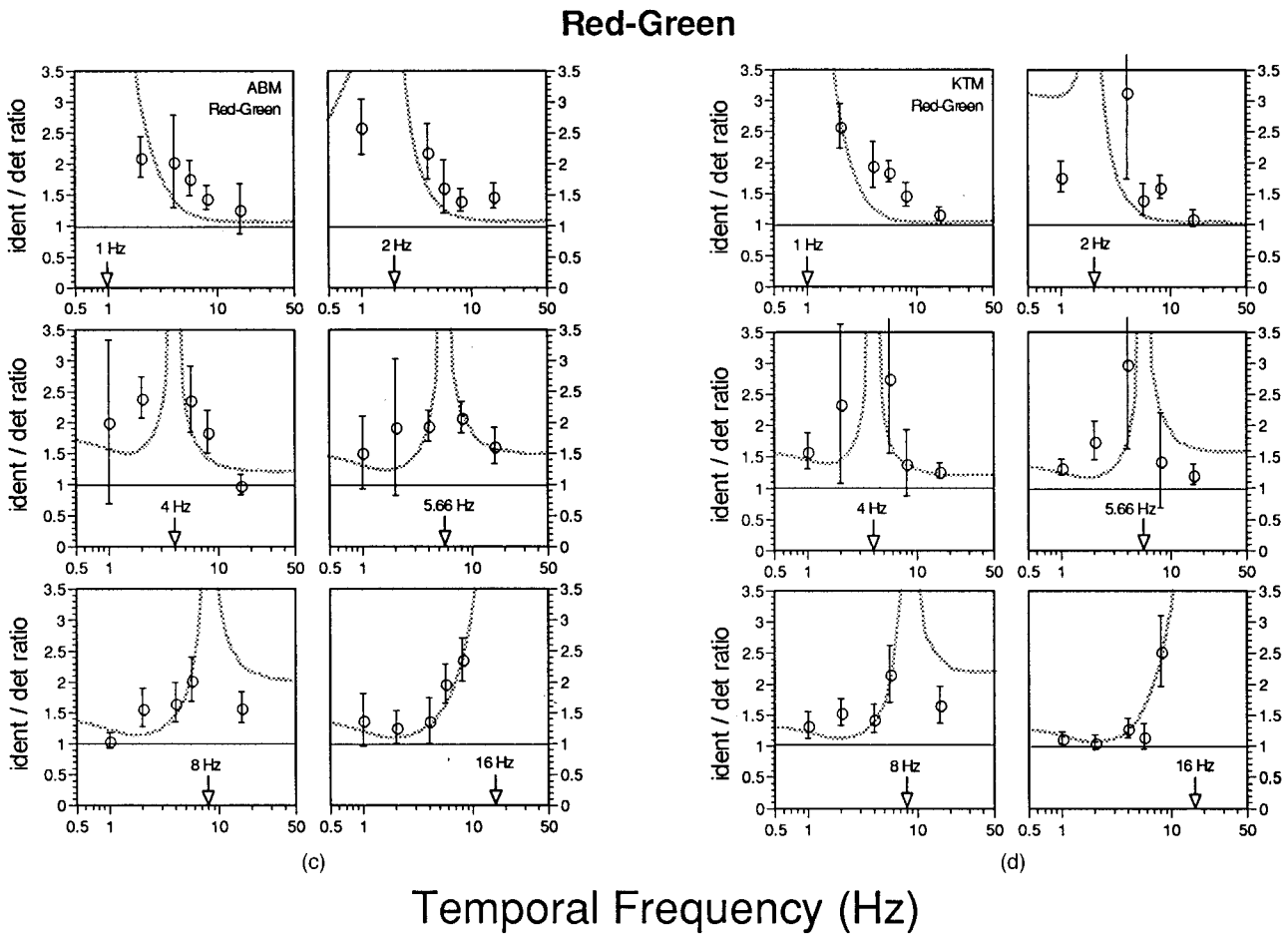

Fig. 3. Identification/detection threshold ratios for each observer with the use of achromatic [(a) and (b)] and isoluminant RG [(c) and (d)] TF pairs. For conditions comparing the flicker frequency, marked by arrows in each plot, the symbols represent the factor by which contrast must be raised above detection threshold to yield 75% correct identification for each compared TF given on the frequency axis. The error bars are standard deviation estimates derived from the detection and identification psychometric function fits. The gray curves represent the model's predictions after parameters were adjusted to give the best fit to both the detection and identification data simultaneously.

The identification/detection threshold ratios found are plotted in Fig. 3. Error bars indicate the calculated standard deviation estimates, which were used in weighting the model fit for each data point. The arrows in each panel indicate the comparison TF, from which the other frequencies along the abscissa had to be correctly identified. The threshold ratio plotted is a measure of how distinguishable two frequencies (e.g., TF1 and TF2) are at low contrast levels. If correct identification is possible at detection threshold, the identification/detection threshold ratio is unity. A threshold ratio of 2.0 for TF2 means that the contrast of TF2 must be raised to twice its 75% detection threshold level before it can be correctly identified as TF2 and not TF1 on 75% of the trials.

As shown by others using achromatic stimuli,[2,37,38] the identification/detection threshold ratio approaches unity for very different frequencies and increases when TF's lie closer together. The data for both observers show that correct identification can occur at detection threshold for each TF tested, as long as the comparison frequencies are sufficiently different. It is interesting to note the 4-Hz data of observer KTM, which show that a 4-Hz achromatic stimulus can be correctly identified at detection threshold contrast from stimuli with both lower and higher TF's. That three categorical regions are evident at detection threshold contrasts has been interpreted previously to indicate the existence of at least three underlying filters,[2,37,38] although we show here that it can also arise within our model framework with a set of only two independent filters. The differences between these interpretations stem from what information each model assumes is available at detection threshold for the identification decision.[1]

The identification/detection threshold ratio for RG TF pairs is shown in Figs. 3(c) and 3(d) for each observer. The same general trends as those for the achromatic stimuli are observed: The threshold ratio is high when TF's lie close together and decreases when the difference between the compared frequencies increases. Although the threshold ratio values are noticeably raised in comparison with those for the achromatic case, the data show that TF identification is possible among RG stimuli at contrasts close to, and in some instances at, detection threshold. Moreover, this identification occurs in the absence of any relative contrast cues, which argues against the operation of a single temporal filter as the basis of

temporal processing in the RG system. Such a system would confound TF and contrast, and hence we model these results by proposing that both detection and TF identification performance rely on the output of two independent linear temporal filters. We also propose that the same strategy applies to both the RG chromatic and luminance systems. The gray curves in Fig. 3 represent the identification performance predicted from the model using two underlying temporal filters in each case by minimizing the total chi-square statistic for both the detection and identification data simultaneously.

B. Two-Filter Model

While the full details of the model can be found in a previous paper,[1] we offer a brief description here. The model considers the tasks of detection and TF identification as two separate, concurrent processes, each drawing on information derived from the outputs of two independent TF-tuned linear filters, with a separate pair subserving chromatic and achromatic vision.

Two linear filters are the minimum number needed to describe the results. The impulse response functions of these filters come from a single family and are temporal derivatives of a Gaussian in log time. The RG chromatic system comprises one filter that is a log-time Gaussian (A) and a second filter (B) that is the first temporal derivative of A. The luminance system uses one filter (A) that is the first derivative and a second filter (B) that is the second derivative of the same generator log-time Gaussian. By deriving filter shapes from the same generator functions in this way, we keep the number of free parameters of the model low (only two parameters, τ and σ, govern the shape of both temporal filters), while ensuring that the filters are an orthogonal set spanning the TF domain. Because we use a pair of filters that are adjacent temporal derivatives, their output magnitudes will also be statistically independent. This allows for efficient coding of TF information and is also a requirement for the mathematics of probability summation, on which we assume that detection performance is based. The absolute sensitivities of each filter (S_A and S_B) are also free parameters of the model.

To model detection performance, we calculate the output of each filter, which is given by the convolution of the stimulus waveform with each filter's impulse response function, and pass this information to a detection unit that calculates detection performance based on (1) probability summation over time and (2) probability summation among the independent filter outputs. The beta exponents used in these calculations are given directly by the average measured Weibull slope parameters of the detection psychometric functions [achromatic: 4.35 $\pm$ 1.53 (KTM), 3.79 $\pm$ 1.56 (ABM), RG: 4.14 $\pm$ 1.49 (KTM), 3.24 $\pm$ 1.19 (ABM)]. Because these did not deviate significantly as a function of TF, both filters are modeled with the same beta exponent, further decreasing the total number of free parameters in the model.

Unlike the labeled-line model proposed by Watson and Robson,[37] our model does not assume that identification performance is contingent on the output of a detection unit. Rather, the orthogonal TF coding of the filters makes it feasible to map the distribution of filter outputs (square of peak amplitude) onto an internal response space and then to use this distribution to classify the TF characteristic of the stimulus. Two points lying close together in this internal response space will arise from very similar TF's and contrasts, and they will be difficult to tell apart. Points lying further apart in this space will be easier to tell apart. In the general line-element theory of discrimination,[2,39–41] it is supposed that an invariant criterion distance (Δ) exists, and if two stimuli lie further apart than this in the space, they have a good chance of being discriminated.

In the paradigm of experiment 1, however, two stimuli are never directly compared. During any trial the observer is shown a single TF and asked to judge whether it was the faster or the slower of the two possibilities. This means that a working memory of frequency patterns must be established, and as each stimulus occurs and gives rise to a pattern of outputs, consideration is given to where it falls with respect to the remembered templates of frequency (see Fig. 8 of Ref. 1). Thus feedback in experiment 1 is useful in order to maintain an up-to-date working memory of the TF's under consideration.

Because the filter output response grows monotonically as a function of contrast, the internal representation of stimuli expands from the origin as contrast is increased. This means that for any two frequencies, the line-element criterion distance Δ can be achieved by increasing the stimulus contrast. The threshold ratio measured in experiment 1 indicates how much contrast needs to be increased above detection threshold in order for this criterion to be met.

In the model, Δ is adjusted along with the two shape and the two sensitivity parameters so that the model predictions are closest to the observed detection and identification data by minimizing chi square. This procedure was carried out iteratively for each data set (each observer's detection and identification data, for the RG and achromatic cardinal stimuli separately) by using Powell's method of numerical minimization.[42] The resulting normalized chromatic and achromatic impulse response functions are shown in Fig. 4 and compared with those obtained previously for 0.25-c/deg stimuli.[1] The best-fitting parameters of the model are given in the caption to Fig. 4.

C. Experiment 2: Temporal-Frequency Discrimination at Suprathreshold Contrast Levels

1. Contrast Response Functions

One choice in the model as it appears in the preceding subsection is the transduction of the linear output of each filter before it enters the internal response space. Squaring the peak filter amplitude improved, in all cases, the fit of the model over that of simple linear transduction and is consistent with the proposed shape of filter transduction at low contrast levels given by other methods.[43–45] Using a peak squaring function also allows us to compare these results with those obtained in an identical fashion at a lower spatial frequency. Freeing the exponent of a common power transducer function improved the fit slightly in some cases, but it was noticed that this parameter was

highly correlated with the size of the line-element criterion distance Δ, while not altering the shape and sensitivity parameters. This suggests that the detection and identification data do not well constrain the transduction aspect of the model and that different performance data collected over an extended contrast range are required to achieve this.

There is considerable support in the literature for the idea that the responses of spatiotemporal filters tuned to different temporal ranges are used as the basis for a metric of velocity coding.[5,7,8,46,47] The exact shape of each filter's contrast response function, and therefore input into the internal response space as modeled in this framework, has important bearings on the predictions of a ratio model that computes speed estimates, especially on those concerning how these estimates might vary with contrast. When the filter outputs all pass through a common power function, response ratios will remain fixed as contrast is varied, and so computed speed estimates will be invariant with contrast.[7]

There are many instances in the literature, however, showing that grating speed perception deviates slightly but significantly from strict contrast invariance[16,17,48] and that this is especially true for slowly moving chromatic gratings.[18,49] Schemes that preserve the ratio model and also incorporate this seeming inconsistency either allow for differential power contrast transduction of the filter outputs before the ratio operation, as suggested by Thompson *et al.*,[20] or, as we propose here, use a Michaelis–Menton contrast response function applied to both RG and achromatic linear filter outputs similarly, before they are projected onto a common internal response space.

According to our model, the transduction properties of the filters affect both the perceived speed and the accuracy of TF discrimination. In experiment 2 we measure TF discrimination over a range of suprathreshold contrasts in order to estimate the shape of the contrast response function. These data allow us to make predictions about the contrast dependency of chromatic and achromatic speed perception. Figure 5 shows RG and achromatic TF discrimination performance for both subjects as a function of contrast above detection threshold. For the RG stimuli (top panels), the contrasts used ranged from twice detection threshold up to the maximum attainable on the CRT while maintaining isoluminance. For the 2-Hz base condition, this was approximately 20 times threshold; it was approximately 8–10 times threshold for the 5.66-Hz base condition. The achromatic contrasts used spanned a greater range, from approximately twice to 40–70 times detection threshold.

Although, in general, observer KTM was able to discriminate finer TF steps than observer ABM in most conditions, the pattern of results as a function of contrast was very similar for the two observers. As contrast increases above threshold, discrimination performance ini-

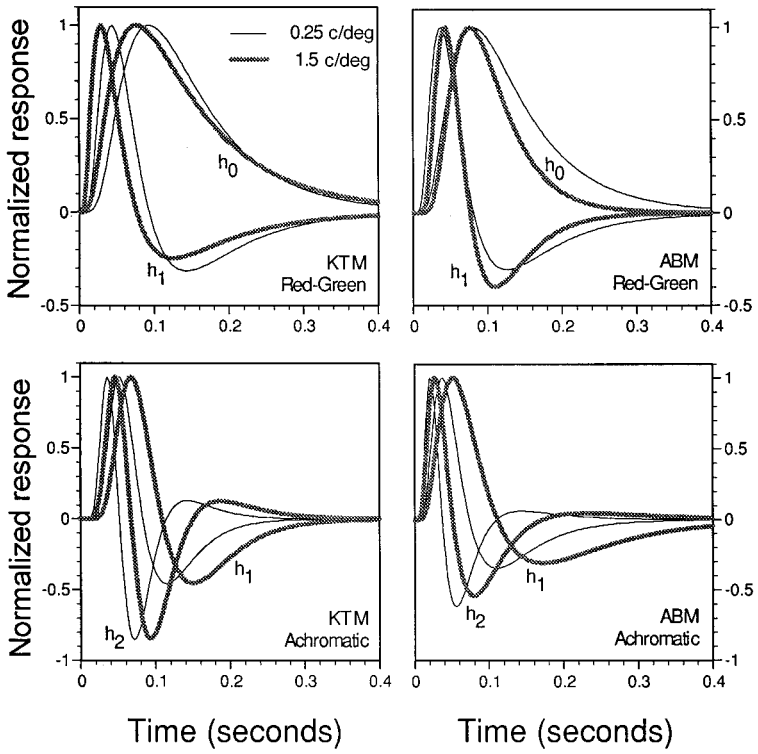

Fig. 4. Normalized impulse response functions corresponding to the two model filters for each observer in the cardinal RG (top) and achromatic (bottom) conditions. The 1.5-c/deg results from experiment 1 are shown by the thick gray curves. For observer KTM the best-fitting model parameters (τ, σ, A_A, A_B, Δ, β) were as follows: for RG conditions, (0.076, 0.972, 8.93, 9.18, 0.1902, 4.14); and for achromatic conditions, (0.108, 0.557, 5.29, 10.10, 0.0550, 4.35). For observer ABM these parameters were as follows: for RG conditions, (0.077, 0.648, 3.84, 4.06, 0.1116, 3.24); and for achromatic conditions, (0.111, 0.822, 2.71, 6.22, 0.0579, 3.79). The RG filters are based on h_0 and h_1, a log-time Gaussian and its first derivative. The achromatic filters, h_1 and h_2, are based on the first and second derivatives of a log-time Gaussian. For comparison, the thin black curves show the inferred impulse response functions taken from a previous paper (Ref. 1) using the same procedure with 0.25-c/deg stimuli.

tially improves very quickly, in accordance with the model presented above. However, the rate of improvement declines at contrasts above approximately four times detection threshold and, at least for the achromatic data, appears to reach an asymptote above approximately ten times threshold. The evidence for saturation of performance in the RG case is equivocal. There is also some indication in the achromatic data of observer KTM that discrimination performance slightly worsens again at the highest contrast level.

2. Modeling the Transducer Function

In the model the linear filter outputs are squared, and discrimination performance is limited by a constant criterion distance between points in an internal response space. Hence TF discrimination performance should continue to increase monotonically with contrast at a rate determined only by the relative sensitivities of the underlying filters as a function of TF. It is evident from Fig. 5 that this does not occur. This signifies that, within the model framework, either Δ grows in some contrast-dependent manner (as would be the case if Δ were proportional to internal noise, which was multiplicative in character) or the filter outputs themselves are transduced such that their responses begin to saturate at high contrast levels. Even though noise in retinal ganglion cells has been found to be additive,[50] there is other neurophysiological evidence showing an increase in response noise with contrast in cortical visually responsive cells.[51] Likewise, there is good evidence that most cells at all levels in the visual system have contrast response functions that are well described by saturating sigmoidal functions.[15] In the event that a combination of these two factors is at play, the effect can nevertheless be modeled by assuming a constant Δ and a saturating transducer function, the output of which represents the effective noise-adjusted signal response as a function of input contrast signal.

We model our TF discrimination results by applying a single Michaelis–Menton transducer function to both the RG and achromatic slow (A) and fast (B) filters. This saturating transducer function has the form

$$\text{Output(input)} = \frac{\text{input}^n}{s^n + \text{input}^n}, \tag{1}$$

where n is an exponent governing the slope of the function and s determines the input required for half-maximal response. Using the impulse response functions inferred from experiment 1, we can calculate the linear output of each underlying temporal filter (A and B) for each data point representing the base TF and the corresponding responses of A and B at TF + ΔTF for each contrast level shown in Fig. 5. We then apply Equation (1) before plotting the transduced filter outputs at TF and TF + ΔTF in the internal response space. This is shown in Fig. 6(a) for the RG data of observer ABM, with the use of a base TF of 2 Hz. Our model requires that Δ, the distance between the representation of TF and TF + ΔTF, be constant across all contrast levels. To determine the transducer function that most nearly results

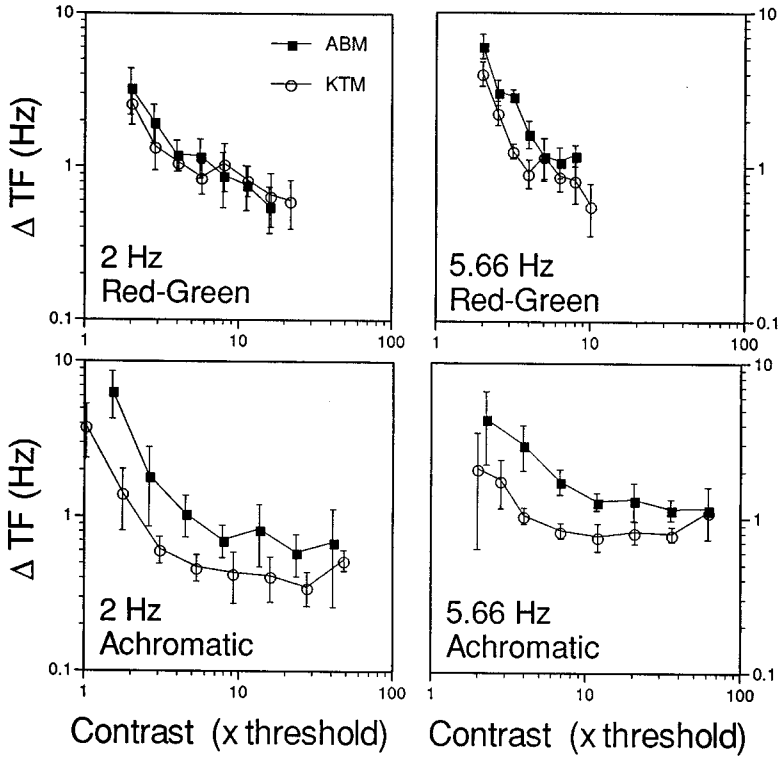

Fig. 5. RG (top) and achromatic (bottom) TF discrimination performance as a function of contrast above detection threshold for each observer from base temporal frequencies of 2 Hz (left) and 5.66 Hz (right). In each trial two stimuli were displayed at equal multiples of detection threshold contrast (± 0.05-$\log_{10}$ unit random contrast jitter), differing only in flicker frequency. For RG stimuli the isoluminance ratio was also adjusted for each TF, in accordance with the results shown in Fig. 1. ΔTF represents the smallest frequency difference from the base TF noticeable by the observer in each case.

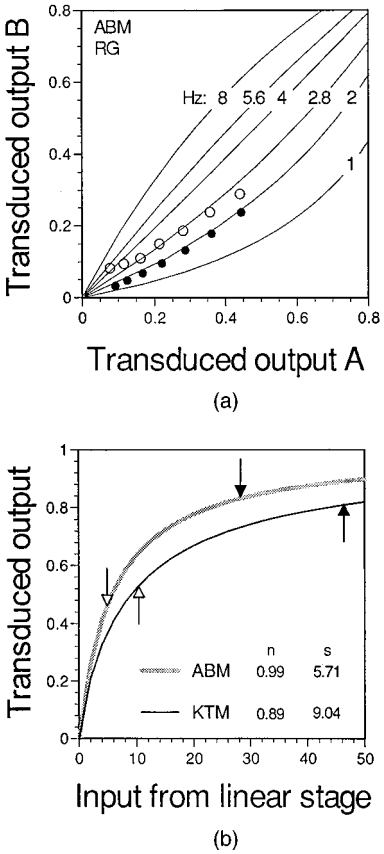

Fig. 6. (a) Representation of the internal response space for observer ABM generated by plotting the transduced output of the model's fast filter (A) against the slow filter (B). The curves radiating from the origin represent the filter output combinations for different flicker rates as indicated over all contrast levels. For clarity, the filled symbols show only the positions in this space of the 2-Hz RG stimuli at the seven contrast levels used in experiment 2. The open symbols indicate the positions in this space of the just-discriminable frequencies (2 + ΔTF Hz) at each corresponding contrast level above detection threshold. The n and s parameters of the Michaelis–Menton transducer function (b) are adjusted so that the distance in this space between the two discriminable frequencies (Δ) is approximately constant at each contrast level for both RG and achromatic stimuli simultaneously. The filled and open arrows indicate the contrast range used in experiment 2 for the achromatic and RG conditions, respectively. Refer to the text for further details.

in this condition, we calculate Δ for each data point and iteratively adjust the parameters (n and s) such that the total coefficient of variation (standard deviation/mean) of Δ is minimized.

In Fig. 6(a) the filled circles show the transduced RG filter responses to the 2-Hz stimuli at the seven different contrast levels used in experiment 2. These data fall on a locus on the curve marked 2 Hz. Loci corresponding to a range of flicker speeds are also shown—we note here that these are not lines in this space, a point that we will return to in Subsection 4.B. The achromatic condition (not shown) follows a very similar pattern, although the loci of constant TF within the range tested do not bend as much as those for the RG condition. The open circles show the filter responses at the higher, just noticeably different frequency TF + ΔTF at contrast levels equated for multiples of threshold. At low contrasts, where TF loci converge (close to the origin), the open circles fall on loci corresponding to higher flicker speeds, following the results shown in Fig. 5. At higher contrast levels, while maintaining a constant line-element distance Δ, the data points representing TF + ΔTF fall on loci closer to the base TF. In this example we note that the loci representing 2 and 2.8 Hz are almost parallel at higher contrast levels, which would reflect a saturation in speed discrimination performance. At the very highest contrast levels, the loci begin to converge. The model would then predict that speed discrimination performance would decline at very high contrast levels. While the RG data never reach these levels, there is some indication of this occurring at high contrasts in the achromatic data of observer KTM. For clarity, only the RG 2-Hz base data are superimposed in Fig. 6(a); however, because we assume a common transducer and internal response space for both RG and achromatic input, the transducer parameters were constrained by considering both the RG and the achromatic data shown in Fig. 5, separately for each observer.

The best-fitting transducer functions for each observer are shown in Fig. 6(b), along with the parameter values of n and s leading to the condition of least variation in Δ. The filled and open arrows in this plot indicate the contrast range used in experiment 2 for the achromatic and the RG condition, respectively. It can be seen that the compressive effects of the saturating function apply mostly in the achromatic condition, which could explain why saturation of discrimination performance was not as evident for the RG data in Fig. 5. The total coefficients of variation in Δ for the fits shown in Fig. 6 were 0.47 for KTM and 0.37 for ABM. As a comparison, when no transducer was applied (linear case), these coefficients were 1.30 and 1.05, respectively. For the simple squaring transducer, these were much worse, at 3.066 and 2.491, respectively. The best-fitting simple power functions resulted in coefficients of 0.517 (exponent 0.36, KTM) and 0.611 (exponent 0.43, ABM).

4. DISCUSSION

A. Red–Green and Achromatic Temporal Filters

One aim of this paper was to reveal how the RG and luminance spatiotemporal contrast sensitivity surfaces are tiled with underlying filters and then to establish filter separability. In order to explain how TF identification performance is not intractably confounded with contrast and also to explain the detection threshold level color identification results, it is necessary to postulate at least two temporal filters for each mechanism responding to isoluminant RG and achromatic stimuli. Figure 4 compares these temporal filters as modeled by our procedure for RG and achromatic stimuli over a sixfold change in spatial frequency. As suggested by earlier studies,[52–54] the time course of the luminance temporal impulse response functions varies with spatial frequency—the filters are proportionately slower at higher spatial frequencies and integrate over longer periods of time. However, as measured by the peak of these response functions, the relative sensitivity of the underlying fast and slow filters remains approximately constant over this spatial-frequency range. In contrast, the time course of the RG

filters remains relatively constant over the same change of spatial frequency, although a small increase in the sensitivity of the slow temporal filter is noted at the coarser spatial scale.

An interesting question that arises from this discussion concerns the site in the visual system of the filtering properties inferred here. In a study of macaque ganglion cell responses to chromatic temporal modulation, Lee *et al.*[30] (their Fig. 4) showed that retinal P cells respond linearly to isoluminant RG modulation with maximal response between 10 and 15 Hz. Moreover, at retinal illuminances of 2000 trolands, these cells are still responsive at 50 Hz. Since this cutoff frequency far exceeds psychophysical measures of RG modulation sensitivity, these authors propose that the limit of temporal resolution for processing RG modulation is set at a later stage than the ganglion cell and that perhaps not all afferent signals to the cortex are utilized for the perceptual tasks of detection and identification.[30] Whether this applies to achromatic information also is uncertain.[55–57] The temporal response properties of lateral geniculate nucleus cells appear to be similar to those of retinal ganglion cells,[55] and while there is some evidence for two distributions of temporal response to achromatic stimuli in monkey V1 and V2,[56] studies addressing the responses of cortical cells to chromatic modulation are only beginning to emerge.[58] Thus we can only posit that the filtering properties that we infer psychophysically include the influence of at least two cortical filters for the RG and luminance systems, although the final results probably reflect filters that operate in cascaded fashion over various stages within the visual pathway.

B. Modeling Speed Perception

We have attempted to define the filtering properties that limit detection performance and permit coding of TF information for flicker and speed in general. Indeed, it is only when this information is provided that an exploration of models for speed coding can proceed. The model presented here uses data collected with flickering stimuli and makes predictions about apparent speed, applicable to both drifting and flickering patterns. The generality of this idea is at variance with a study that the marked relative slowing of high-contrast 2-Hz drifting RG patterns is not as evident in the 2-Hz flickering case.[59] Clearly, the relationship between perceived flicker and drift speed needs further exploration in order to assess this general aspect of the speed coding model. As well as accounting for the empirical finding that RG isoluminant stimuli appear to drift more slowly compared with achromatic stimuli moving at the same physical rate, a successful model must also explain the contrast dependency of perceived speed. While the deviations from contrast independence are relatively minor in real terms, they are of interest here because they have been shown to be different for RG and achromatic stimuli, depending on the speeds being compared.

Thompson[16] initially reported that the perceived speed of achromatic gratings is not strictly contrast invariant but apparent speed increases with increasing contrast for slowly drifting patterns. On the other hand, the opposite was found for quickly drifting 2-c/deg patterns—the crossover of effects occurring at drift rates of 8 Hz, or 4 deg/s.[16] In a later paper, Stone and Thompson[17] failed to replicate the latter effect, instead finding that over a wide range of spatiotemporal configurations (3 c/deg at 8.25 and 10 Hz, giving speeds of 2.75 and 3.3 deg/s, respectively), perceived speed always increased with increasing contrast, and that the result was independent of spatial frequency. More recently, Hawken *et al.*[18] confirmed that increasing contrast results in higher perceived speed for slowly drifting (1 c/deg at 1 Hz) RG and achromatic stimuli. In addition, they reported a small but consistent decrease in apparent speed with increasing contrast for fast-moving gratings (1 c/deg at 8 Hz), in keeping with Thompson's original findings. This effect was shown with the use of achromatic gratings in all four of their observers, and three of these subjects also showed a similar effect for RG gratings.[18] Contrast-dependent speed perception is also seen in the data of Mullen and Boulton,[14] who matched the speed of a drifting RG grating with a variable-speed achromatic grating.

Based on the finding that the dependency of speed on contrast (speed gain) was considerably stronger for the 1-Hz drifting RG patterns than for the achromatic gratings, and relatively similar for the 8-Hz patterns, Hawken *et al.* proposed that there was a single pathway that handled motion processing of luminance and chromatic targets at high TF's but separate pathways for RG and luminance stimuli at low TF's.[18,19] Instead, all these results may be explained by the simple model that we

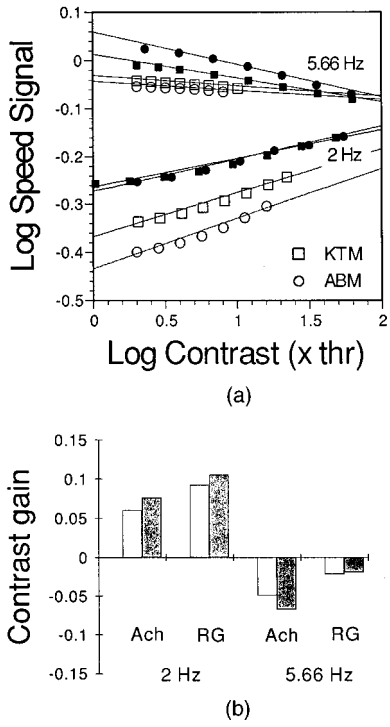

Fig. 7. (a) Predicted speed as a function of contrast given by the ratio model. The filled symbols represent the predicted achromatic speeds, and the open symbols represent predicted RG speeds for observers KTM (squares) and ABM (circles). The lines are best-fitting linear regressions through the predictions. (b) Slopes of the best-fitting linear regressions in (a), equivalent to the speed gain in each condition (2- and 5.66-Hz base speeds), for observers KTM (open bars) and ABM (filled bars).

propose here. Referring to Fig. 6(a), we note that because of the nonlinear transduction of filter outputs, the response ratio of the two filters changes as a function of contrast, resulting in iso-TF loci that are not lines in the internal response space. According to a simple ratio model, speed is coded as the angle in this space. The resulting predictions of the ratio model for speed, and how this changes with contrast, are shown in Fig. 7(a). To facilitate comparison with Hawken *et al.*,[18] we plot predicted speed and contrast above threshold on log–log axes for both observers. The filled symbols represent the predicted achromatic speeds, and the open symbols represent RG speeds.

Figure 7(a) shows that the model predicts that RG stimuli generate smaller speed signals than similar achromatic patterns moving at the same rate and also that the shortfall in chromatic speed becomes less at higher drift rates, in accordance with the results observed by Cavanagh *et al.*[13] The slope of the contrast–speed relationships in this plot is equivalent to the speed gain defined by Hawken *et al.*[18] The lines drawn in Fig. 7(a) are linear regressions through the data. The slopes of these regressions are shown in Fig. 7(b). The highest speed gain is afforded the slow RG stimuli, followed by the slow achromatic stimuli for both observers. The model predicts that fast RG and achromatic patterns have a negative speed gain; they will slow down with increasing contrast. This is exactly the same pattern of results as that observed by Hawken *et al.*[18] Thus the existence of different contrast gains for perceived speed at different TF's, or for chromatic versus achromatic stimuli, need not be an indication of separate motion mechanisms, as has been previously suggested.[18,19]

The success of the ratio model account that we give here supports the idea that both color information and luminance information are processed in a common manner and site and that differences between color and luminance speed perceptions are mainly due to differences in front-end temporal filtering properties coupled with a saturating contrast response function. This is consistent with psychophysical studies showing that even at low speeds, color-induced and luminance-induced motion aftereffects can interact with both color-defined and luminance-defined nulling signals,[60] and also with the observation that adding chromatic modulation to luminance stimuli can act to reduce apparent speed.[13] Finally, the nonlinear transduction stage in our model also provides a simple, physiologically realistic, and unifying account of how the perceived speed dependency on contrast can change as a function of the base comparison speed.

ACKNOWLEDGMENTS

This research was supported by a Medical Research Council research grant MT-0819. We thank Eric Fredericksen for many invaluable discussions concerning temporal-frequency coding and modeling aspects of this paper.

Address all correspondence to Andrew B. Metha, Center for Visual Science, Room 274, Meliora Hall, University of Rochester, Rochester, New York 14627-0270; tel: 716-273-4719; fax: 716-271-3043; e-mail: andrewm@cvs.rochester.edu.

REFERENCES

1. A. B. Metha and K. T. Mullen, "Temporal mechanisms underlying flicker detection and identification for red–green and achromatic stimuli," J. Opt. Soc. Am. A **13**, 1969–1980 (1996).
2. M. B. Mandler and W. Makous, "A three channel model of temporal frequency perception," Vision Res. **24**, 1881–1887 (1984).
3. R. F. Hess and R. J. Snowden, "Temporal properties of human visual filters: number, shapes and spatial covariation," Vision Res. **32**, 47–59 (1992).
4. S. T. Hammett and A. T. Smith, "Two temporal channels or three? A re-evaluation," Vision Res. **32**, 285–291 (1992).
5. P. Thompson, "The coding of velocity of movement in the human visual system," Vision Res. **24**, 41–45 (1984).
6. S. J. Anderson and D. C. Burr, "Spatial and temporal selectivity of the human motion detection system," Vision Res. **25**, 1147–1154 (1985).
7. E. H. Adelson and J. R. Bergen, "Spatio-temporal energy models for the perception of motion," J. Opt. Soc. Am. A **2**, 284–299 (1985).
8. A. T. Smith and G. K. Edgar, "Antagonistic comparison of temporal frequency filter outputs as a basis for speed perception," Vision Res. **34**, 253–265 (1994).
9. N. V. S. Graham, *Visual Pattern Analysers*, Oxford Psychology Series 16 (Oxford U. Press, New York, 1989).
10. M. A. Losada and K. T. Mullen, "The spatial tuning of chromatic mechanisms identified by simultaneous masking," Vision Res. **34**, 331–341 (1994).
11. M. A. Losada and K. T. Mullen, "Color and luminance spatial tuning estimated by noise masking in the absence of off-frequency looking," J. Opt. Soc. Am. A **12**, 250–260 (1995).
12. J. Yang and W. Makous, "Spatiotemporal separability in contrast sensitivity," Vision Res. **34**, 2569–2576 (1994).
13. P. Cavanagh, C. W. Tyler, and O. E. Favreau, "Perceived velocity of moving chromatic gratings," J. Opt. Soc. Am. A **1**, 893–899 (1984).
14. K. T. Mullen and J. C. Boulton, "Absence of smooth motion perception in color vision," Vision Res. **32**, 483–488 (1992).
15. G. Sclar, J. H. R. Maunsell, and P. Lennie, "Coding of image contrast in central visual pathways of the macaque monkey," Vision Res. **30**, 1–10 (1990).
16. P. G. Thompson, "Perceived rate of movement depends on contrast," Vision Res. **22**, 377–380 (1982).
17. L. Stone and P. Thompson, "Human speed perception is contrast dependent," Vision Res. **32**, 1535–1549 (1992).
18. M. J. Hawken, K. Gegenfurtner, and C. Tang, "Contrast dependence of colour and luminance motion mechanisms in human vision," Nature (London) **367**, 268–270 (1994).
19. K. Gegenfurtner and M. J. Hawken, "Perceived velocity of luminance, chromatic, and non-Fourier stimuli: influence of contrast and temporal frequency," Vision Res. **36**, 1281–1290 (1996).
20. P. G. Thompson, L. S. Stone, and S. Swash, "Speed estimates from grating patches are not contrast-normalized," Vision Res. **36**, 667–674 (1996).
21. A. B. Metha, "Detection and direction discrimination in terms of post-receptoral mechanisms," Ph.D. dissertation (The University of Melbourne, Melbourne, Australia, 1994).
22. A. B. Metha, A. J. Vingrys, and D. R. Badcock, "Calibration of a color monitor for visual psychophysics," Behav. Res. Methods Instrum. Comput. **25**, 371–383 (1993).
23. H. L. DeVries, "The heredity of the relative numbers of red and green receptors in the human eye," Genetica (The Hague) **24**, 199–212 (1948).
24. J. Pokorny, Q. Jin, and V. C. Smith, "Spectral-luminosity functions, scalar linearity, and chromatic adaptation," J. Opt. Soc. Am. A **10**, 1304–1313 (1993).

25. C. F. Stromeyer III, R. E. Kronauer, A. Ryu, A. Chapparo, and R. T. Eskew, Jr, "Contributions of human long-wave and middle-wave cones to motion detection," J. Physiol. (London) **485**, 221–243 (1995).
26. D. Regan and C. W. Tyler, "Some dynamic features of color vision," Vision Res. **11**, 1307–1324 (1971).
27. P. Cavanagh, D. I. A. MacLeod, and S. M. Anstis, "Equiluminance: spatial and temporal factors and the contribution of blue-sensitive cones," J. Opt. Soc. Am. A **4**, 1428–1438 (1987).
28. W. H. Swanson, T. Ueno, V. C. Smith, and J. Pokorny, "Temporal modulation sensitivity and pulse detection thresholds for chromatic and luminance perturbations," J. Opt. Soc. Am. A **4**, 1992–2005 (1987).
29. P. Kaiser, M. Ayama, and R. L. P. Vimal, "Flicker photometry: residual minimum flicker," J. Opt. Soc. Am. A **3**, 1989–1993 (1986).
30. B. B. Lee, J. Pokorny, V. C. Smith, P. R. Martin, and A. Valberg, "Luminance and chromatic modulation sensitivity of macaque ganglion cells and human observers," J. Opt. Soc. Am. A **7**, 2223–2236 (1990).
31. B. B. Lee, T. Yeh, J. Kremers, V. C. Smith, and J. Pokorny, "The central filter acting upon parvocellular pathway signals," Invest. Ophthalmol. Visual Sci. Suppl. **34**, 912 (1993).
32. V. C. Smith, B. B. Lee, J. Pokorny, P. R. Martin, and A. Valberg, "Responses of macaque ganglion cells to the relative phase of heterochromatically modulated lights," J. Physiol. (London) **458**, 191–221 (1992).
33. V. C. Smith, J. Pokorny, M. Davis, and T. Yeh, "Mechanisms subserving temporal modulation sensitivity in silent-cone substitution," J. Opt. Soc. Am. A **12**, 241–249 (1995).
34. K. T. Mullen and J. J. Kulikowski, "Wavelength discrimination at detection threshold," J. Opt. Soc. Am. A **7**, 733–742 (1990).
35. A. B. Metha, A. J. Vingrys, and D. R. Badcock, "Detection and discrimination of moving stimuli: the effects of color, luminance and eccentricity," J. Opt. Soc. Am. A **11**, 1697–1709 (1994).
36. K. T. Mullen, "The contrast sensitivity of human colour vision to red–green and blue–yellow chromatic gratings," J. Physiol. (London) **359**, 381–400 (1985).
37. A. B. Watson and J. G. Robson, "Discrimination at threshold: labelled detectors in human vision," Vision Res. **21**, 1115–1122 (1981).
38. R. F. Hess and G. T. Plant, "Temporal frequency discrimination in human vision: evidence for an additional mechanism in the low spatial and high temporal frequency region," Vision Res. **25**, 1493–1500 (1985).
39. J. J. Vos, "Line elements and physiological models of color vision," Color Res. Appl. **4**, 208–216 (1979).
40. B. A. Wandell, "Measurement of small color differences," Psychol. Rev. **89**, 281–302 (1982).
41. H. R. Wilson, "Responses of spatial mechanisms can explain hyperacuity," Vision Res. **26**, 453–469 (1986).
42. W. H. Press, B. P. Flannery, S. A. Teukolsky, and W. T. Vetterling, *Numerical Recipes in C: The Art of Scientific Computing* (Cambridge U. Press, Cambridge, 1988).
43. G. E. Legge, "A power law for contrast discrimination," Vision Res. **21**, 457–467 (1981).
44. J. Gottesman, G. S. Rubin, and G. E. Legge, "A power law for perceived contrast in human vision," Vision Res. **21**, 791–799 (1981).
45. D. Laming, "Theoretical basis of the processing of simple visual stimuli," in *Vision and Visual Dysfunction, Limits of Vision*, J. J. Kulikowski, V. Walsh, and I. J. Murray, eds. (CRC Press, Boca Raton, Fla., 1991), Vol. 5, pp. 23–34.
46. M. G. Harris, "Velocity specificity of the flicker to pattern sensitivity ratio in human vision," Vision Res. **20**, 687–691 (1980).
47. A. Johnston and C. W. G. Clifford, "A unified account of three apparent motion illusions," Vision Res. **35**, 1109–1123 (1995).
48. P. Thompson and L. S. Stone, "Contrast dependence of speed perception: effects of temporal presentation," Invest. Ophthalmol. Visual Sci. Suppl. **33**, 973 (1992).
49. K. T. Mullen and J. C. Boulton, "Interactions between colour and luminance contrast in the preception of motion," Ophthalmic Physiol. Opt. **12**, 201–205 (1992).
50. L. J. Croner, K. Purpura, and E. Kaplan, "Response variability in retinal ganglion cells of primates," Proc. Natl. Acad. Sci. USA **90**, 8128–8130 (1993).
51. D. J. Tolhurst, J. A. Movshon, and I. D. Thompson, "The dependence of response amplitude and variance of cat visual cortical neurones on stimulus contrast," Exp. Brain Res. **41**, 405–418 (1981).
52. D. H. Kelly, "Theory of flicker and transient responses. II. Counterphase gratings,"J. Opt. Soc. Am. A **61**, 632–640 (1971).
53. D. J. Tolhurst, "Reaction times in the detection of gratings by human observers: a probabilistic mechanism," Vision Res. **15**, 1143–1149 (1975).
54. A. B. Watson and J. Nachmias, "Patterns of temporal interaction in the detection of gratings," Vision Res. **17**, 893–902 (1977).
55. A. M. Derrington and P. Lennie, "Spatial and temporal contrast sensitivities of neurones in lateral geniculate nucleus of macaque," J. Physiol. (London) **357**, 219–240 (1984).
56. K. H. Foster, J. P. Gaska, M. Nagler, and D. A. Pollen, "Spatial- and temporal-frequency selectivity of neurones in visual cortical areas V1 and V2 of the macaque monkey," J. Physiol. (London) **365**, 331–363 (1985).
57. B. B. Lee, P. R. Martin, and A. Valberg, "Sensitivity of macaque retinal ganglion cells to chromatic and luminance flicker," J. Physiol. (London) **414**, 223–243 (1989).
58. M. J. Hawken, R. M. Shapley, and D. H. Grosof, "Temporal frequency tuning of neurones in macaque V1: effects of luminance contrast and chromaticity," Invest. Ophthalmol. Visual Sci. Suppl. **33**, 955 (1992).
59. G. B. Henning and A. M. Derrington, "Speed, spatial-frequency, and temporal-frequency comparisons in luminance and colour gratings," Vision Res. **34**, 2093–2101 (1994).
60. A. M. Derrington and D. R. Badcock, "The low level motion system has both chromatic and luminance inputs," Vision Res. **25**, 1879–1884 (1985).